Aldol product 23b was prepared from **21** and isobutyraldehyde (**13b**) in 60% yield: IR ($CDCl_3$) 3450, 3045, 3020, 2955, 1920, 1665, 1595, 1490, 1450, 1352, 1230 cm^{-1}; ^1H NMR (360 MHz, $CDCl_3$) δ 7.43-7.26 (m, 10 H), 4.31 (t, 1 H), 2.92 (d, 1 H), 2.39 (s, 3 H), 1.97 (m, 1 H), 0.88 (dd, 6 H); ^{13}C NMR (360 MHz, $CDCl_3$) δ 213.4, 199.7, 134.1, 128.8, 128.4, 128.3, 113.2, 103.0, 75.4, 32.9, 28.0, 19.7, 17.9; CIMS *m/e* (relative intensity) 307 (MH^+, 20), 289 (100), 23 4 (31), 191 (18); HRMS exact mass calcd for $C_{21}H_{23}O_2$ (MH^+) 307.1698, found 307.1712.

Aldol product 23d was prepared from **21** and benzaldehyde (**13d**) in 50% yield: IR ($CDCl_3$) 3390, 3040, 3018, 2960, 2900, 1920, 1660, 1590, 1485, 1445, 1235 cm^{-1}; ^1H NMR (360 MHz, $CDCl_3$) δ 7.35-7.01 (m, 15 H), 5.80 (s, 1 H), 3.62 (br, 1 H), 2.37 (s, 3 H); ^{13}C NMR (360 MHz, $CDCl_3$) δ 213.7, 199.4, 141.3, 133.9, 128.7, 128.6, 128.3, 128.3, 128.21, 128.18, 128.0, 127.6, 126.4, 115.6, 115.0, 71.8, 27.9; CIMS *m/e* (relative intensity) 341 (MH^+, 6), 323 (100), 235 (94), 191 (36), 105 (16); HRMS exact mass calcd for $C_{24}H_{21}O_2$ (MH^+ 341.1542, found 341.1534.

Aldol product 23f was prepared from **21** and acetophenone (**13f**) in 35% yield: IR ($CDCl_3$) 3460, 3040, 3020, 2920, 1920, 1662, 1593, 1490, 1448, 1355, 1260, 1245 cm^{-1}; ^1H NMR (250 MHz, $CDCl_3$) δ 7.45-7.21 (m, 15 H), 5.08 (s, 1 H), 2.35 (s, 3 H), 1.67 (s, 3 H); ^{13}C NMR (63 MHz, $CDCl_3$) δ 212.8, 201.0, 147.4, 129.0, 128.9, 128.5, 128.5, 128.4, 128.1, 128.1, 126.8, 124.5, 116.3, 115.1, 76.6, 30.5, 28.6; FAB *m/e* (relative intensity) 355 (MH^+, 8), 319 (12), 295 (24), 234 (100), 191 (23), 121 (27); HRMS exact mass calcd for $C_{25}H_{23}O_2$ (MH^+) 355.1698, found 355.1696.

Acknowledgment. Support by the donors of the Petroleum Research Fund of the American Chemical Society (20838-G1, 23475-AC), by the American Cancer Society (CH 525), and by the National Institutes of Health (RO1-GM 45970) is gratefully acknowledged.

Supplementary Material Available: ^1H and ^{13}C NMR spectra of compounds **11, 16a, 16b, 16c, 16d, 16e, 23a, 23b, 23d,** and **23f** (10 pages). Ordering information is given on any current masthead page.

$Ni_{23}Se_{12}(PEt_3)_{13}$. An Intramolecular Intergrowth of NiSe and Ni

J. G. Brennan,† T. Siegrist, Y.-U. Kwon, S. M. Stuczynski, and M. L. Steigerwald*

Contribution from the AT&T Bell Laboratories, 600 Mountain Avenue, Murray Hill, New Jersey 07974. *Received January 9, 1992*

Abstract: The reaction of $Ni(COD)_2$ (COD = cyclooctadiene) with Et_3PSe at elevated temperature gives a mixture of Ni_3Se_2 and elemental Ni. When the same reagents are combined at lower temperature the cluster compound $Ni_{23}Se_{12}(PEt_3)_{13}$ is formed and can be isolated as a crystalline solid. We have determined the structure of this compound crystallographically (trigonal space group *R3c*, a = 17.577 (1) Å, c = 75.191 (6) Å, V = 20118 Å^3, Z = 6). The crystallography shows the cluster to be a fusion of distorted fragments of NiSe (NiAs structure type) and hexagonally close packed elemental Ni. This cluster can be converted thermally to the same solid products (Ni_3Se_2 and Ni) as those resulting from the combination of Ni^0 and Se^0 under the more forcing conditions. This shows that the cluster is allowable as an intermediate in the molecules-to-solids conversion.

Introduction

We report that bis(cyclooctadiene)Ni, $Ni(COD)_2$, reacts with triethylphosphine selenide, Et_3PSe, in refluxing toluene to give a mixture of extended solids, Ni_3Se_2 and elemental Ni. We also report the synthesis, structure, and thermal behavior of $Ni_{23}Se_{12}(PEt_3)_{13}$, **1**, a molecular cluster compound we have been able to isolate from the reaction of the two zerovalent[1] precursor molecules. We analyze the structure of **1** in relation to extended solid-state compounds and see that it can be viewed as a fusion of a molecular fragment of NiSe and a molecular fragment of Ni. In this way we show that the title compound is a molecular example of a solid-state intergrowth compound.

We have shown previously that inorganic solid-state tellurides can result from the reaction of low-valent transition-metal complexes with trialkylphosphine tellurides[2] and have seen that such reactions can be arrested at the molecular stage. In the particular case of nickel telluride[2c] we found that two cluster intermediates can be isolated, $Ni_9Te_6(PEt_3)_8$ and $Ni_{20}Te_{18}(PEt_3)_{12}$, and that each cluster can be identified with a fragment of the NiTe structure. We suggested that in such simple solid-forming reactions the structure of the solid is mimicked very early on in the growth process. To test this hypothesis we examined the reaction of Ni^0 with triethylphosphine selenide.

Experimental Section

Unless noted to the contrary all operations were conducted under an inert atmosphere using standard drybox and Schlenk techniques. All solvents were anhydrous grade, used as purchased from Aldrich. Bis(cyclooctadiene)nickel was either prepared using literature methods[3] or purchased from Strem Chemicals and used as received. Triethylphosphine (Aldrich) and selenium (Alfa) were used as received. Triethylphosphine selenide was prepared by the action of triethylphosphine on selenium. Powder X-ray diffraction patterns were recorded on a Rigaku Miniflex diffractometer (Cu Kα).

Preparation of Ni- and Se-Containing Solid-State Compounds. $Ni(COD)_2$ (0.28 g, 1.0 mmol) was dissolved in 15 mL of toluene and Et_3PSe (0.20 g, 1.0 mmol) was dissolved in 5 mL of toluene. The Se-containing solution was added to the Ni-containing solution, and the resulting mixture was heated at reflux 17 h. The mixture was cooled and filtered to give a black solid (90.0 mg). This solid did not diffract X-rays. A portion of this solid (53 mg) was heated at 270 °C for 18 h. This gave a shiny black solid (45 mg). Powder X-ray diffraction showed this to be Ni_3Se_2 with small interferences due to elemental Ni.

Preparation of $Ni_{23}Se_{12}(PEt_3)_{13}$. $Ni(COD)_2$ (2.46 g, 9.0 mmol) was suspended in toluene (50 mL) to which PEt_3 (0.2 mL, 1.7 mmol) had been added. In a separate vessel Et_3PSe (6.71 g, 34.1 mmol) was dissolved in toluene (100 mL). The solution of Et_3PSe was diluted with heptane (100 mL), taking care that the phosphine selenide remained in

† Present address: Department of Chemistry, Rutgers University, P.O. Box 939, Piscataway, NJ 08855-0939.

(1) Austad, T.; Rød, T.; Åse, K.; Sonstad, J.; Norbury, A. H. *Acta Chem. Scand.* **1973**, *27*, 1939.

(2) (a) Steigerwald, M. L.; Rice, C. E. *J. Am. Chem. Soc.* **1988**, *110*, 4228. (b) Steigerwald, M. L. *Chem. Mater.* **1989**, *1*, 52. (c) Brennan, J. G.; Siegrist, T.; Stuczynski, S. M.; Steigerwald, M. L. *J. Am. Chem. Soc.* **1989**, *111*, 9240. (d) Brennan, J. G.; Siegrist, T.; Stuczynski, S. M.; Steigerwald, M. L. *J. Am. Chem. Soc.* **1990**, *112*, 9233. (e) Steigerwald, M. L.; Siegrist, T.; Stuczynski, S. M. *Inorg. Chem.* **1991**, *30*, 2256. (f) Steigerwald, M. L.; Siegrist, T.; Stuczynski, S. M. *Inorg. Chem.* **1991**, *30*, 4940. (g) Steigerwald, M. L.; Siegrist, T.; Stuczynski, S. M.; Kwon, Y.-U. *J. Am. Chem. Soc.* **1992**, *114*, 3155.

(3) Schunn, R. A. *Inorg. Synth.* **1974**, *15*, 5.

0002-7863/92/1514-10334$03.00/0

Table I. Crystallographic Data for $Ni_{23}Se_{12}(PEt_3)_{13}$

empirical formula	$Ni_{23}Se_{12}P_{13}$[a]
formula weight	2700.5
crystal system	trigonal
space group	$R3c$
a	17.577 (1) Å
c	75.191 (6) Å
V	20118 (2) Å^3
a_{rh}	27.040 (2) Å
α_{rh}	37.9°
Z	6
T	23 °C
$F(000)$	11460
ρ_{calc}	1.337 g/cm^3
μ	8.90 mm^{-1}
λ	1.54056 Å Cu kα
crystal dimensions (rhombohedral cell)	0.12 × 0.12 × 0.12 mm
$2\theta_{max}$	138°
transmission factors	0.36–0.54
scan type	$\theta/2\theta$
data collected	$0 \le h \le 18, 0 \le k \le 18, 0 \le l \le 90$
no. of reflcns	20643
no. of unique reflcns	8215
no. of reflcns, $I_{net} > 2.52\sigma(I_{net})$	6220
no. of parameters	145
R_f[b]	0.082
R_w[c]	0.161
secondary extinction coeff	0.075 (5)

[a] Not all of the carbon atoms were located. See text. [b] $R_f = \{\sum(F_o - F_c)\}/\{\sum F_o\}$. [c] $R_w = \{\sum w(F_o - F_c)^2\}/\{\sum(wF_o^2)\}$.

solution. The $Ni(COD)_2$ suspension was added to the Et_3PSe solution via pipette, and the mixture was stirred at room temperature overnight after which point the mixture was filtered. This solution deposited crystalline solid over the space of 2 weeks at room temperature. The supernatant liquor was removed, and the solid was washed with pentane to give the dark, crystalline product (0.22 g, 15%). Elemental Anal. Found (calculated for $Ni_{23}Se_{12}P_{13}C_{78}H_{195}$): C, 24.16 (24.44); H, 4.95 (5.13); Ni, 34.95 (35.22); P, 10.26 (10.50); Se, 24.80 (24.70).

Crystallographic Study of $Ni_{23}Se_{12}(PEt_3)_{13}$. Crystals which were suitable for X-ray diffraction were selected and loaded in Lindemann capillaries in a He-filled drybox, and the capillaries were sealed. Diffraction data were collected on Enraf-Nonius CAD4 diffractometers equipped with graphite monochromatized Mo Kα and Cu Kα radiation. All calculations were performed on a MicroVAX II computer using the NRCVAX crystal structure system.[4] Gaussian integration absorption corrections were applied. Refinement procedures have been described elsewhere.[5] Hydrogen atoms were not included in the refinements. A summary of the crystallographic results is given in Table I.

Two sets of data were collected. The first used Mo Kα radiation. The structure of the core of the cluster was solved using this data set however, this set had a large number of reflections unobserved, and therefore not all of the carbon atoms could be located. For this reason the second data set, this time using Cu Kα radiation, was collected. With this second data set 69 of the 78 carbon atoms could be located. The inclusion of the located carbon atoms in the solution did improve the refinement (with the 69 C atoms the R values were lower ($R_f = 0.050$, $R_w = 0.049$) than without them ($R_f = 0.082$, $R_w = 0.161$)), but since we could not locate all of the carbon atoms we included only the cluster core in the final refinement. By only including the cluster core, our final model accounts for 1247 of the 1910 electrons in **1**. This results in the high R values shown in Table I. Compound **1** crystallizes in the space group $R3c$, and the absolute configuration was determined.

The values of interatomic distances within the core of **1** is given in Table II, and a list of selected interatomic angles is given in Table III. Complete crystallographic information, including the parameters for the carbon atoms which were located, is given in the supplementary material.

Thermal Conversion of $Ni_{23}Se_{12}(PEt_3)_{13}$ to Ni_3Se_2 and Ni. $Ni_{23}Se_{12}(PEt_3)_{13}$ (172 mg, 0.045 mmol) was sealed in an evacuated Pyrex tube and heated at 300 °C for 2 h, after which time the tube was cooled and opened. The resulting black solid was washed (pentane) and dried (99 mg, 96% mass recovery based on complete removal of PEt_3). Powder X-ray diffraction shows Ni_3Se_2 with weak signals due to elemental Ni.

Table II. Selected Bond Distances in **1**[a]

		Ni_1	
Ni_2	2.524 (3)	Ni_4	2.566 (5)
Ni_3	2.532 (5)	Ni_5	2.544 (5)
		Ni_2	
Ni_3	2.429 (3)	Ni_6	2.544 (4)
$Ni_{3'}$	2.606 (3)	Se_1	2.371 (3)
Ni_4	2.481 (4)	Se_2	2.338 (4)
Ni_5	2.584 (4)	Se_3	2.371 (3)
		Ni_3	
Ni_4	2.485 (3)	Se_1	2.384 (3)
Ni_5	2.590 (4)	Se_2	2.330 (3)
Ni_7	2.553 (4)	Se_3	2.356 (3)
		Ni_4	
$Ni_{4'}$	2.346 (6)	Ni_8	2.644 (4)
Ni_6	2.457 (3)	Se_4	2.337 (3)
Ni_7	2.456 (3)		
		Ni_5	
$Ni_{5'}$	2.831 (6)	P	2.227 (4)
Se_1	2.303 (3)		
		Ni_6	
Ni_7	2.768 (4)	Se_3	2.449 (3)
Ni_8	2.614 (4)	Se_4	2.477 (3)
Se_2	2.362 (3)	P	2.21 (1)
		Ni_7	
Ni_8	2.615 (3)	Se_4	2.461 (3)
Se_2	2.350 (3)	P	2.214 (3)
Se_3	2.470 (3)		
		Ni_8	
Ni_9	2.594 (3)	$Se_{4'}$	2.464 (3)
Se_3	2.385 (3)	P	2.271 (4)
Se_4	2.473 (3)		
		Ni_9	
Se_4	2.433 (1)	P	2.268 (7)

[a] Numbering as in Figure 1; primed and unprimed subscripts denote symmetry-equivalent atoms. Distances in Å.

Table III. Selected Bond Angles in **1**[a]

Ni_2–Ni_1–Ni_3	57.4 (2)	Se_1–Ni_5–$Se_{1'}$	161.7 (2)
Ni_2–Ni_1–$Ni_{3'}$	62.1 (2)	Se_2–Ni_6–Se_3	111.5 (2)
Ni_4–Ni_1–$Ni_{4'}$	54.4 (2)	Se_2–Ni_6–Se_4	109.1 (1)
Ni_5–Ni_1–$Ni_{5'}$	67.6 (2)	Se_3–Ni_6–Se_4	112.1 (1)
Se_1–Ni_2–Se_2	132.7 (2)	Se_2–Ni_7–Se_3	110.4 (2)
Se_1–Ni_2–Se_3	99.0 (1)	Se_2–Ni_7–Se_4	110.1 (1)
Se_2–Ni_2–Se_3	115.3 (2)	Se_3–Ni_7–Se_4	112.3 (1)
Se_1–Ni_3–Se_2	132.8 (2)	Se_3–Ni_8–Se_4	114.8 (1)
Se_1–Ni_3–Se_3	99.0 (1)	Se_3–Ni_8–$Se_{4'}$	114.9 (1)
Se_2–Ni_3–Se_3	115.3 (2)	Se_4–Ni_8–$Se_{4'}$	114.8 (1)
$Ni_{4'}$–Ni_4–Ni_6	115.2 (2)	Se_4–Ni_9–$Se_{4'}$	117.4 (1)
$Ni_{4''}$–Ni_4–Ni_6	172.0 (2)		
$Ni_{4'}$–Ni_4–Ni_7	171.7 (2)		
$Ni_{4''}$–Ni_4–Ni_7	115.3 (1)		
Ni_6–Ni_4–Ni_7	68.6 (1)		

[a] Numbering as in Figure 1; primed and unprimed subscripts denote symmetry-equivalent atoms. Angles in deg.

Results

The reaction of $Ni(COD)_2$ with $SePEt_3$ in refluxing toluene deposits a black solid (67% mass recovery based on complete precipitation of Ni and Se) that is amorphous by X-ray diffraction. Heating this powder results in the crystallization of the solid. X-ray diffraction then shows the solid to be a mixture of Ni_3Se_2[6] and elemental Ni. This solid-forming process is not as effective as the corresponding Ni/Te case. There we found the quantitative

(4) (a) Le Page, J.; White, P. S.; Gabe, E. J. *Proc. Am. Cryst. Assoc. Annual Meeting*, 1986; Hamilton, Canada, AlP: New York, 1986; Poster PA23. (b) Gabe, E. J.; Lee, F. L.; Le Page, J. In *Crystallographic Computing 3*; Sheldrick, G. H., Krüger, C., Goddard, R., Eds.; Clarendon Press: Oxford, UK, 1985; p 163.

(5) Siegrist, T.; Schneemeyer, L. F.; Sunshine, S. A.; Waszczak, J. V. *Mater. Res. Bull.* **1988**, *23*, 1429.

production and deposition of crystalline NiTe[2c] directly from refluxing toluene with no evidence for the formation of elemental Ni. It is easy to rationalize the difference between the two cases. The P–Se bond in the phosphine selenide is stronger than the P–Te bond in the phosphine telluride, and therefore the phosphine selenide is more reluctant to surrender the Se atom to the growing solid.

We attempted to isolate molecular compounds from the reaction of $SePEt_3$ with $Ni(COD)_2$ in order to further characterize the processes by which the entended solids are formed. Since the P–Se bond is stronger than the corresponding P–Te bond, and in view of our results in the Ni/Te system we reasoned that $SePEt_3$ should be used in excess and that free PEt_3 should be kept to a minimum. The combination of $Ni(COD)_2$, $SePEt_3$, and PEt_3 in a 1:3.8:0.15 ratio in toluene/heptane (3:2 by volume) at room temperature gave the cluster compound $Ni_{23}Se_{12}(PEt_3)_{13}$, **1**, as a pure, black crystalline solid (eq 1).

$$Ni(COD)_2 + SePEt_3 \rightarrow Ni_{23}Se_{12}(PEt_3)_{13} \qquad (1)$$

Subsequent higher temperature thermolysis of **1** liberated the phosphine quantitatively and gave a solid whose powder X-ray diffraction pattern was the same as that resulting from the high-temperature reaction of $Ni(COD)_2$ and $SePEt_3$. These results establish a connection between **1** and the solid-state products, Ni_3Se_2 and Ni.

The constitution of **1** was established by elemental analysis and single crystal X-ray crystallography. Elemental analysis of **1** is consistent with the formulation $Ni_{23}Se_{12}(PEt_3)_{13}$, and the crystallography established the structure shown in Figure 1. Crystallographic data are given in Tables I–III. In addition, powder X-ray diffraction of samples of the solid product of eq 1 show only peaks due to **1**.

There is extensive Ni–Se and Ni–Ni bonding within the cluster. There are 57 Ni–Se distances less than 2.5 Å (r_{av} = 2.39 Å). This average is in the range of Ni–Se interatomic distances reported in solid-state Ni/Se compounds (2.37 Å in Ni_3Se_2,[6a] 2.50 Å in NiSe[6b]) and previously reported Ni/Se molecular cluster compounds.[7] There are 63 Ni–Ni distances in **1** that are less than 2.8 Å, 45 of which are less than 2.6 Å and 18 of which are less than 2.5 Å. The shortest Ni–Ni internuclear distance is 2.35 Å. Within the set of 63 distances the average Ni–Ni separation is 2.55 Å. This is slightly longer than the distance in elemental Ni (2.49 Å). Based on internuclear distances there is no direct Se–Se bonding within the cluster.

The molecule has a 3-fold symmetry axis which is defined by Ni1 and Ni9, and the crystal is polar. Several Ni/Se cluster compounds have been reported recently, notably those prepared by Fenske and co-workers.[7]

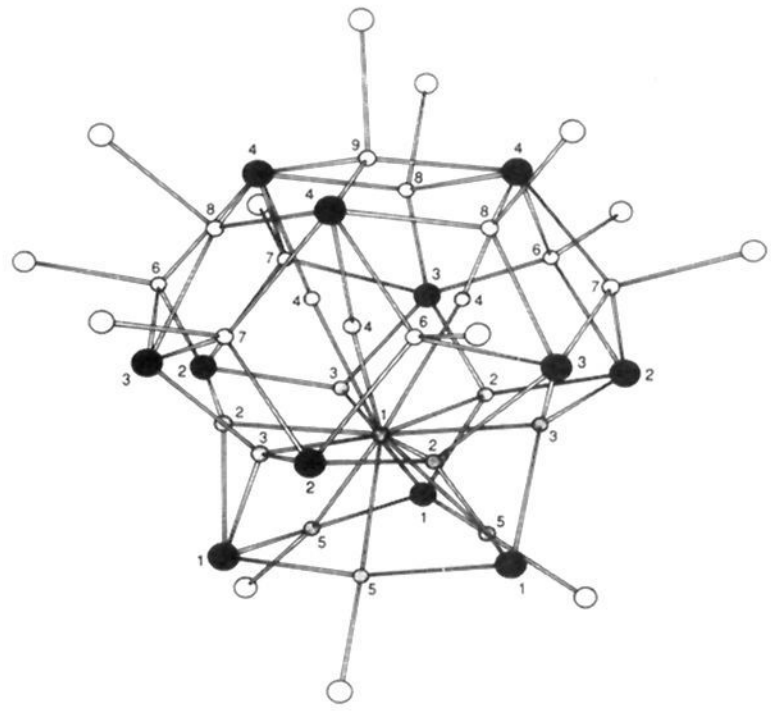

Figure 1. The structure of $Ni_{23}Se_{12}(PEt_3)_{13}$. Filled circles represent Se atoms. Open circles represent phosphorus atoms (the carbon and hydrogen atoms of the phosphine ligands have been omitted). The shaded circles represent Ni atoms. The stippled Ni atoms (Ni1–Ni5) are associated in the text with the hcp Ni structure; the striped Ni atoms (Ni6–Ni9) are associated with the NiSe structure. Atoms having the same number are symmetry-equivalent, related by the 3-fold axis defined by Ni1 and Ni9.

Discussion

We believe that it is useful to compare the structure of **1** to that of related extended solids[8] for at least four reasons. First the structure of **1** is curious. We did not predict the structure of **1** in advance of the crystallography. It will be valuable to the synthesis chemistry of clusters to be able to make such a priori predictions. One step along this long road is to view the cluster in terms of the simpler extended solids. To the extent that structural correlations exist they will provide guidelines for the prediction of the structures of large molecular clusters. It is clear that there are cases in which such correlations are quite compelling,[8b,9] cases where such correlations do not exist, and cases in which the reconstructions required to change from the solid structure to the cluster structure are extreme but nonetheless identifiable.[2e,f]

A second reason for comparing the structures of clusters to those of extended solids relates to the mechanisms by which molecules are converted to solids. Since **1** can be converted thermally to a mixture of Ni_3Se_2 and Ni there exists an easy reaction pathway from **1** to those solids. Structural comparisons between the endpoints of this path will help elucidate the very complicated chemical process.

A third reason for the cluster/solid comparison is the study of structure-property relationships. It is hoped that the physical properties of the extended solids and those of the large clusters can be correlated. An appreciation of the properties of one will amplify that of the other provided that the relationships between the solid and the cluster are understood in sufficient detail. Correlations of this type are becoming widely accepted for semiconductor nanoclusters.[10]

A fourth reason for viewing larger molecular clusters in solid-state terms is synthetic in motivation. One problem which hampers research in nanoscale materials is the inability to prepare perfectly monodisperse materials.[10] One approach to the solution of this problem is to use "molecular" synthesis chemistry to make larger and larger crystalline molecular clusters. The connection to nanoscale materials research is made most directly when the internal structure of the molecular clusters begins to mimic that of related extended solids. To the extent that this occurs this variety of synthesis chemistry will be directly applicable to nanocluster research.

The feature of **1** that is most obviously related to elemental Ni is the central Ni atom (Ni 1). It is 12 coordinate, each coordinated atom being Ni. The distances from Ni1 to these other Ni atoms are between 2.52 and 2.56 Å, with the average distances being 2.55 Å. This should be compared to the internuclear distance in elemental Ni which is 2.49 Å. Ni1 is central to an almost planar hexagon that is defined by three Ni2 atoms and three Ni3 atoms. This seven atom array is capped above by a triangle of Ni4 atoms

(6) (a) Stevels, A. L. N. *Philips Res. Repts. Suppl.* **1969**, *9*, 1. (b) Grønvold, F.; Jacobsen, E. *Acta Chem. Scand.* **1956**, *10*, 1440.

(7) (a) Fenske, D.; Ohmer, J.; Hachengenei, J. *Angew. Chem., Int. Ed. Engl.* **1985**, *24*, 993. (b) Fenske, D.; Hollnagel, A. *Angew. Chem., Int. Ed. Engl.* **1989**, *28*, 1390. (c) Fenske, D.; Ohmer, J. *Angew. Chem., Int. Ed. Engl.* **1987**, *26*, 148. (d) Fenske, D.; Hollnagel, A.; Merzweiler, K. *Angew. Chem., Int. Ed. Engl.* **1988**, *27*, 965. (e) Fenske, D.; Krautscheid, H.; Müller, M. *Angew. Chem., Int. Ed., Engl.* **1992**, *31*, 321. (f) McConnachie, J. M.; Ansari, M. A.; Ibers, J. A. *J. Am. Chem. Soc.* **1991**, *113*, 7078. (g) See, also: Hong, M.; Huang, Z.; Liu, H. *J. Chem. Soc., Chem. Commun.* **1990**, 1210.

(8) For related discussions, see: (a) Dance, I. G. *Polyhedron* **1986**, *5*, 1037. (b) Lee, S. C.; Holm. R. H. *Angew. Chem., Int. Ed. Engl.* **1990**, *29*, 840. (c) Krebs, B.; Henkel, G. *Angew. Chem., Int. Ed. Engl.* **1991**, *30*, 769.

(9) For examples of structural similarities between clusters and solids, see: (a) Christou, G.; Hagen, K. S.; Bashkin, J. K.; Holm, R. H. *Inorg. Chem.* **1985**, *24*, 1010. (b) Saito, T.; Yamamoto, N.; Nagase, T.; Tsuboi, T.; Koyabashi, K.; Yamagata, T.; Imoto, H.; Unoura, K. *Inorg. Chem.* **1990**, *29*, 764.

(10) (a) Steigerwald, M. L.; Brus, L. E. *Ann. Rev. Mat. Sci.* **1989**, *19*, 471. (b) Steigerwald, M. L.; Brus, L. E. *Acct. Chem. Res.* **1990**, *23*, 183.

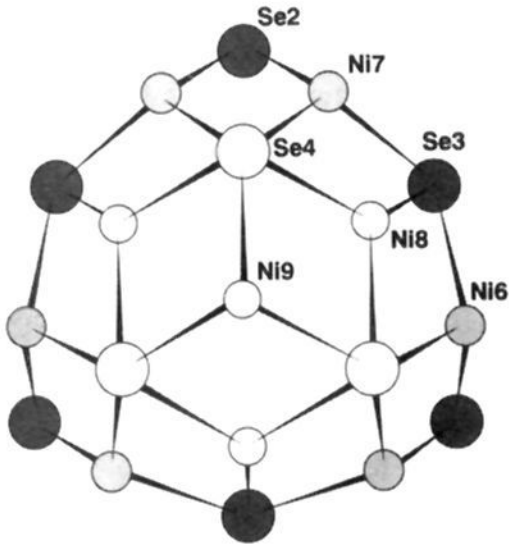

Figure 2. The cluster fragment $Ni_{10}Se_9$ resulting from the removal of the Ni_{13} core and the capping agents (phosphine ligands and the three Se1 atoms) from **1**. This is the view down the 3-fold axis, i.e., in the plane of the page of Figure 1.

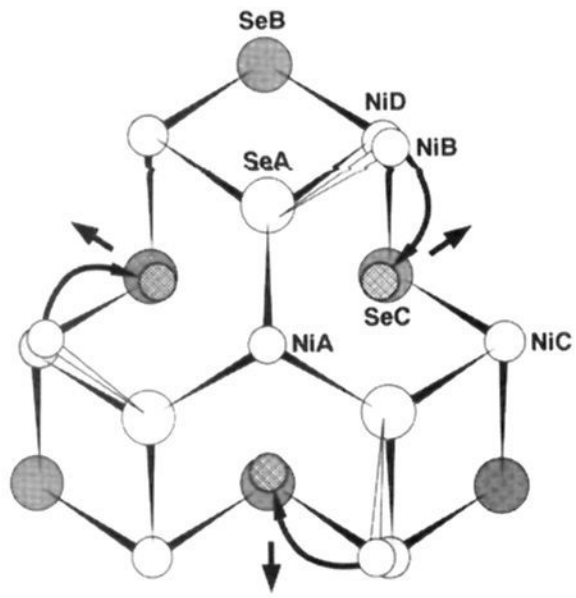

Figure 3. A segment, $Ni_{10}Se_9$, of NiAs-type NiSe, viewed down the *c*-axis. The arrows indicate the atomic displacements that are required to transform this fragment of NiSe to the $Ni_{10}Se_9$ fragment of **1**. The crosshatched circle represents the position occupied by NiB after such a displacement.

and below by a triangle of Ni5 atoms. The two capping triangles (Ni4 and Ni5) are eclipsed when viewed down the normal axis, i.e., the 3-fold symmetry axis. This disposition of **13** atoms is that of hexagonal close-packing, hence the core of **1** can be idealized as a fragment of hexagonally close-packed Ni. Note tht bulk Ni forms a face-centered cubic solid rather that a hexagonally close-packed solid. The latter structure has been observed only in thin films.[11] Reduced dimensionality apparently favors hexagonal close packing of Ni atoms.

If one removes the central 13 Ni atoms and the three Se1 atoms which cap the bottom of the Ni_{13} array and ignores the capping phosphine ligands, there remains a fragment of stoichiometry $Ni_{10}Se_9$. This fragment is shown in Figure 2. The fragment shows 3-fold symmetry. This is reminiscent of the symmetry of the NiAs structure type.[12] This is relevant because stoichiometric NiSe forms in the NiAs structure.[6b]

In Figure 3 we show a $Ni_{10}Se_9$ fragment of NiSe. The *c*-direction is perpendicular to the page. The drawing shows four atomic layers along the *c*-axis: the top Ni layer (four Ni atoms, NiA and three NiB), the upper Se layer to which these Ni atoms are bonded (three Se atoms represented as large open circles, SeA), the lower Ni layer (six Ni atoms, three NiC, and three NiD), and

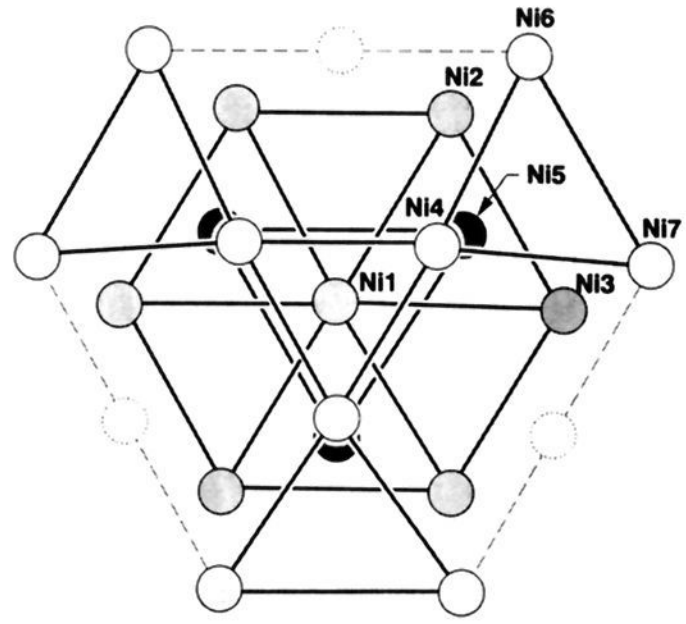

Figure 4. The 19 Ni atom array in **1** defined by Ni1, 3 Ni2, 3 Ni3, 3 Ni4, 3 Ni5, 3 Ni6, and 3 Ni7. The view is from the same point as in Figure 2. The darkened circles represent atoms in the lowest plane, shaded circles represent atoms in the middle plane, and open circles represent atoms in the upper plane. The dotted circles represent three Ni atoms which would continue the array of hcp Ni.

the bottom Se layer (six Se atoms represented as large filled circles, SeC). This fragment was chosen by examining the NiSe structure, looking for structural similarities between it and the $Ni_{10}Se_9$ piece of **1** shown in Figure 2. The two directing features are the 3-fold axis and the on-axis Ni atom.

Comparison of Figures 2 and 3 uncovers a number of similarities between **1** and NiSe in addition to the local 3-fold symmetry: Ni9 is symmetrically bonded to three Se4 atoms in Figure 2 as NiA is bonded to SeA in Figure 3. Each Se4 is bonded below to one Ni6 and one Ni7 in Figure 2 as each SeA is bonded below to one NiC and one NiD in Figure 3. Each Se2 in Figure 2 is bonded above to one Ni6 and one Ni7 as each SeB in Figure 3 is bonded above to one NiC and one NiD. The Se4–Ni6–Se2–Ni7 connectivity in Figure 2 is similar to the SeA–NiC–SeB–NiD connectivity in Figure 3.

There are two major differences between the fragments pictured in Figures 2 and 3. These differences are suggested by the arrows in Figure 3. If NiB in Figure 3 is moved to the position of the small gray circle, the position and connectivity of NiB would be that of Ni8 in Figure 2. Similarly if SeC were moved radially outward as suggested by the arrow in Figure 3 its position and connectivity would be that of Se3 in Figure 2. From this analysis we conclude that the $Ni_{10}Se_9$ upper half of **1** is a reconstructed fragment of NiSe[13] Since the Ni_{13} fragment of **1** defined by Ni1 through Ni5 is identified as a piece of hcp Ni, we suggest that **1** be viewed as a molecule-sized hybrid[14] of the two solids NiSe and Ni: the top half of the molecule being NiSe and the bottom half being Ni.

The physical connection between the NiSe half and the Ni half of the cluster is then an intramolecular example of a heteroepitaxial interface.[15] In a heteroepitaxial crystal growth process a solid of one composition grows on a solid of a second composition in such a way that crystallinity is maintained across the interface between the two compositions. The process necessarily implies matching of the two different crystal lattices. It is easy to see the lattice matching in **1**. In Figure 4 we show a 19 Ni atom subset of **1**, taken directly from the crystallographically determined structure. The figure shows that six of the Ni atoms (three Ni6 and three Ni7) that we identified above as members of the NiSe fragment are also members of the hcp Ni structure. To emphasize

(11) (a) *Gmelin Handbuch der Anorganische Chemie*; Verlag Chemie GMBH: Weinheim, 1967; Ni All-1, 108. (b) Morimoto, H.; Sakata, H. *J. Phys. Soc. Jpn.* **1962**, *17*, 136.

(12) Useful descriptions of the NiAs structure are included in the following texts. (a) West, A. R. *Solid State Chemistry and Its Applications*; John Wiley & Sons: Chichester, UK, 1984. (b) Wells, A. F. *Structural Inorganic Chemistry*; Clarendon Press, Oxford, UK, 1984.

(13) Alternatively the $Ni_{10}Se_9$ unit can be seen as an essentially undistorted Ni_7Se_9 fragment of the NiSe structure that has been capped by three Ni atoms. These three "extra" Ni atoms are placed in the high coordination sites on the surface of the Ni_7Se_9 fragment.

(14) In a sense this is a molecular version of a solid state intergrowth compound. See, for example: Rao, C. N. R.; Gopalakrishnan, J. *New Directions in Solid State Chemistry*; Cambridge University Press: Cambridge, UK, 1986; p 248 et seq.

(15) Reference 14, see also p 228 of that volume.

this we include in Figure 4 three Ni atoms that are not in **1** but that would be present were the ideal hcp Ni crystal to continue[16] We conclude that the interface between the NiSe portion of **1** and the Ni portion of **1** is exactly the six Ni atoms that are common to both.

Note that the Ni–Ni bonds in the central Ni_{13} unit of the cluster are on average longer than Ni–Ni bonds in elemental Ni. It is more common for the lattice parameters of nanoclusters of extended solids to be smaller than the corresponding values for those solids. This is usually explained by invoking the surface tension of the solid generating a "Laplace pressure" which compresses the cluster to give shorter internal bond distances. The equivalent chemical explanation is that the otherwise unsatisfied valences on the surface of the cluster are satisfied by surface reconstructions which cause compression of the internal lattice. In the case of **1** the bonding sites external to the Ni_{13} core are satisfied by the NiSe cap (in addition to the three Se1 atoms and three phosphine ligands which cap the bottom of the cluster), thus the compression of the Ni_{13} core to a density higher than that of Ni is avoided. In other words, the lattice matching between the Ni core and the NiSe shell force a net expansion of the internal Ni lattice.

The cluster **1** shows structural features of both NiSe and Ni, while the solid-state products of its thermolysis include Ni_3Se_2 and not NiSe. The path by which **1** disproportionates to give the observed solids presumably, although not necessarily, involves the interdiffusion of the two halves of **1**. The details of the disproportionation are certainly quite complicated and merit further study. Of similar complexity is the route by which **1** is formed from Ni and Se. It is interesting to speculate whether **1** is formed by the fusion of the "Ni-half" and the "NiSe-Half" or by the assembly of some other different sets of atoms or fragments.

(16) The layered description of the Ni_{19} core of **1** is similar to that shown by Teo and co-workers for Au- and Ag-based clusters: Teo, B. K.; Zhang, H.; Shi, X. *J. Am. Chem. Soc.* **1990**, *112*, 8552.

Conclusions

We have shown that $Ni(COD)_2$ reacts with $SePEt_3$ at elevated temperature to give a mixture of Ni_2Se_2 and Ni, that the two combine at lower temperature to give the cluster **1**, and that **1** gives a similar mixture of Ni_3Se_2 and Ni on heating. We have determined the structure of **1** and analyzed it in terms of associated extended solids, showing it to be a molecular example of an intergrowth of NiSe and Ni. We have characterized the interface between the two members of the intergrowth, showing that interface to be six Ni atoms which are included in both the NiSe and Ni substructures.

Supplementary Material Available: Positional parameters for **1** (Table S1), thermal parameters for **1** (Table S2), complete list of interatomic distances and angles for **1** (Table S3), crystallographic data for inclusion of C atoms (Table S5), positional parameters for **1** including located C atoms (Table S6), and thermal parameters for **1** including located C atoms (Table S7) (11 pages); table of observed and calculated structure factors (Table S4) (55 pages). Ordering information is given on any current masthead page.

Calculation and Electronic Description of Quadratic Hyperpolarizabilities. Toward a Molecular Understanding of NLO Responses in Organotransition Metal Chromophores

David R. Kanis, Mark A. Ratner,* and Tobin J. Marks*

Contribution from the Department of Chemistry and Materials Research Center, Northwestern University, Evanston, Illinois 60208-3113. *Received May 18, 1992*

Abstract: This contribution explores the use of the computationally efficient, chemically-oriented INDO electronic structure model (ZINDO) in concert with perturbation theory to relate molecular quadratic hyperpolarizabilities to molecular architecture and electronic structure in transition metal chromophores. The ZINDO-derived second-order nonlinear optical responses are found to be in excellent agreement with the experiment for a variety of ferrocenyl and (arene)chromium tricarbonyl derivatives. The assumptions needed to describe nonlinear optical response in simple molecular orbital terms are presented, and their reliability is analyzed in a quantitative fashion. All of the ferrocenyl chromophores examined are found to closely resemble traditional organic π-electron chromophores in that intense MLCT transitions dominate the second-order response. A detailed examination of the modest second-order nonlinearities of the chromium arenes identifies two shortcomings that may be characteristic of many organometallic architectures: the intrinsic hyperpolarizability may be far greater than the experimentally accessible vectorial component of β (that directed along the dipole moment direction), and the electronic distribution about the metal centers in many organometallic structures is pseudo-centrosymmetric. This explains the relatively low nonlinearities of a number of recently reported organometallic chromophores. The design utility of the present computational formalism is illustrated by the calculation of the second-order response of a hypothetical organometallic chromophore having a very acentric electron distribution and, correspondingly, a larger calculated second-order response than any measured to date for an organometallic chromophore.

Introduction

Substances that exhibit highly nonlinear optical (NLO) responses are currently of great scientific and technological interest.[1] While inorganic solids such as $LiNbO_3$ and KH_2PO_4 have traditionally been the NLO materials of widest interest, recent results suggest that molecule-based macroscopic π-electron ensembles possess many superior NLO characteristics. Specifically, molecule-based NLO materials offer ultrafast response times, lower dielectric constants, better processability characteristics (e.g., amenability to thin-film fabrication), and enhanced nonresonant NLO responses relative to the traditional inorganic solids.[2] Since

* Authors to whom correspondence should be addressed at the Department of Chemistry.

(1) (a) Boyd, R. W. *Nonlinear Optics*; Academic Press: New York, 1992. (b) Prasad, N. P.; Williams, D. J. *Introduction to Nonlinear Optical Effects in Molecules and Polymers*; Wiley: New York, 1991. (c) Eaton, D. F. *Science* **1991**, *253*, 281–287. (d) Marder, S. R.; Beratan, D. N.; Cheng, L.-T. *Science* **1991**, *252*, 103–106. (e) Heeger, A. J., Orenstein, J., Ulrich, D. R., Eds. Nonlinear Optical Properties of Polymers. *Mater. Res. Soc. Symp. Proc.* **1988**, *109*. (f) Zyss, J. *J. Mol. Electron.* **1985**, *1*, 25–56. (g) Williams, D. J. *Angew. Chem., Int. Ed. Engl.* **1984**, *23*, 690–703. (h) Shen, Y. R. *The Principles of Nonlinear Optics*; Wiley: New York, 1984.

0002-7863/92/1514-10338$03.00/0